Ninth International Conference on
THIN-WALLED STRUCTURES – ICTWS2023
Sydney, Australia, Nov 29 – Dec 1, 2023

DISTORTIONAL BUCKLING OF COLD-FORMED STEEL CHANNELS UNDER MINOR AXIS BENDING

Shuhao Ma and John Papangelis

School of Civil Engineering, University of Sydney, Australia
e-mails: shma8904@uni.sydney.edu.au, john.papangelis@sydney.edu.au

Keywords: Distortional buckling; Cold-formed steel; Channel; Minor axis; Finite element; Non-linear analysis.

Abstract. *The direct strength method (DSM) is an alternative design method to the effective width method in calculating the bending moment capacity of cold-formed steel members. The DSM uses elastic buckling moments with an appropriate strength curve to calculate the design moment capacity and avoids tedious plate by plate calculations to determine the effective width. However, the current DSM design equations have been calibrated for channel and zed sections under major axis bending and may not be appropriate for cold-formed steel channels under minor axis bending. In this paper, elastic finite strip buckling analysis and non-linear finite element analysis on cold-formed steel channels under minor axis bending with the lips in compression are described. The elastic finite strip buckling analysis is used to investigate the buckling modes while the non-linear finite element analysis calculates the ultimate moment for these members. The aim is to compare the ultimate moments calculated by the non-linear finite element analysis with the current DSM and, if necessary, derive a new DSM design equation for cold-formed steel channels under minor axis bending with the lips in compression.*

1 INTRODUCTION

The direct strength method (DSM) in AS/NZS 4600 [1] and AISI S100 [2] is an alternative design method to the effective width method in calculating the bending moment capacity of cold-formed steel members. The DSM was first developed by Schafer and Pekoz [3] based on earlier research by Hancock *et al*. [4] on distortional buckling. The DSM uses elastic buckling moments with an appropriate strength curve to calculate the design moment capacity and avoids tedious plate by plate calculations to determine the effective width. However, the current DSM design equations have been calibrated for channel and zed sections under major axis bending and may not be appropriate for channels under minor axis bending.

This issue has been partially addressed by Oey and Papangelis [5] who derived a new DSM design equation for local buckling of channels under minor axis bending with the web in compression. However, there appears to be very little research on investigating the design moment capacity for channels under minor axis bending with the lips in compression.

The longitudinal stress distribution in a channel under minor axis bending with the lips in compression is shown in Figure 1. While the lips are in uniform compression, the flanges are subjected to a stress gradient and the web is in uniform tension. Because the channel section is unsymmetric under minor axis bending, first yield occurs in the lips for this type of loading.

An elastic buckling analysis is usually required to determine the governing failure modes for cold-formed steel members under various loading conditions. Such an analysis can be efficiently performed by computer programs such as THIN-WALL-2 [6] and CUFSM [7] which employ the finite strip method of analysis [8]. Theoretical equations for the elastic distortional buckling stress for lipped flanges under uniform stress caused by major axis bending have been derived by Hancock [9] and Schafer *et al*. [10]. Glauz [11] developed an

analytical method to calculate the elastic distortional buckling stress for lipped flanges under stress gradient caused by minor axis bending as shown in Figure 1.

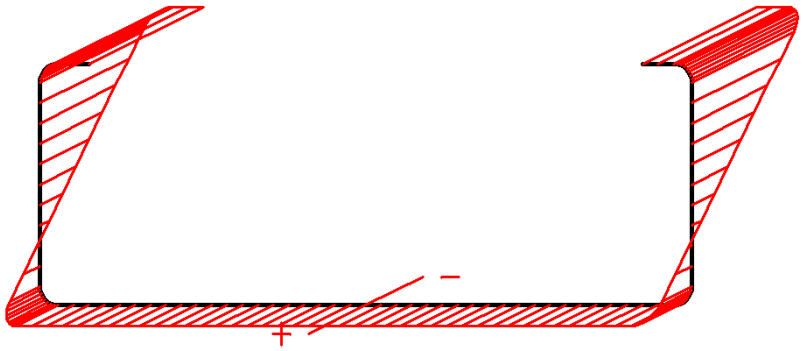

Figure 1: Longitudinal stress distribution in channel under minor axis bending.

While there has been much research in confirming the current DSM design equations for cold-formed steel channels under major axis bending with testing and finite element analysis [12-14], research on channels under minor axis bending is very limited. Martins *et al.* [15] reported numerical results on the ultimate moment capacities for several cross-sections failing by distortional buckling, including inverted hat sections with the outward facing lips in compression. Fan *et al.* [16] tested stainless steel channels under minor axis bending with the web in compression and derived a new DSM design equation. Oey and Papangelis [5] used a non-linear finite element analysis (NLFEA) to calculate the ultimate moments for cold-formed steel channels under minor axis bending with the web in compression and derived a new DSM design equation. Glauz and Schafer [17] and Glauz [18] derived a general form of the DSM design equation for local and distortional buckling of cold-formed steel members unsymmetric about the axis of bending. However, it is unclear if their DSM design equation for distortional buckling is applicable for channel sections because the equation is based on test results of complex hat sections.

In this paper, elastic finite strip buckling analysis and NLFEA on cold-formed steel channels under minor axis bending with the lips in compression are described. The elastic finite strip buckling analysis is performed by the program THIN-WALL-2 [6]. The NLFEA is performed by the commercial finite element analysis program Strand7 [19]. The aim is to compare the ultimate moments calculated by the NLFEA with the current DSM design equation for distortional buckling and, if necessary, derive a new DSM design equation for cold-formed steel channels under minor axis bending with the lips in compression.

2 GEOMETRY

Figure 2 shows the channel dimension nomenclature, where D is the section depth, B is the flange width, L is the lip width, R is the inside corner radius and t is the material thickness. For this investigation, all of the standard Australian cold-formed steel channels were analysed plus additional created channels were also analysed so as to cover a wider range of section slenderness $\sqrt{(M_y/M_{od})}$, where M_y is the yield moment and M_{od} is the elastic distortional buckling moment calculated from THIN-WALL-2.

The section slenderness of the standard Australian cold-formed steel channels is in the range 0.73 to 1.56 while the additional created channels had a range of 0.24 to 2.0. Channels with depths D ranging from 100-400 mm and thicknesses t ranging from 0.75-7.0 mm were analysed. The ratio of section depth to flange width D/B ranged from 2.0 to 3.39 while the ratio of flange width to lip width B/L ranged from 1.80 to 5.33. A total of 90 channels were analysed.

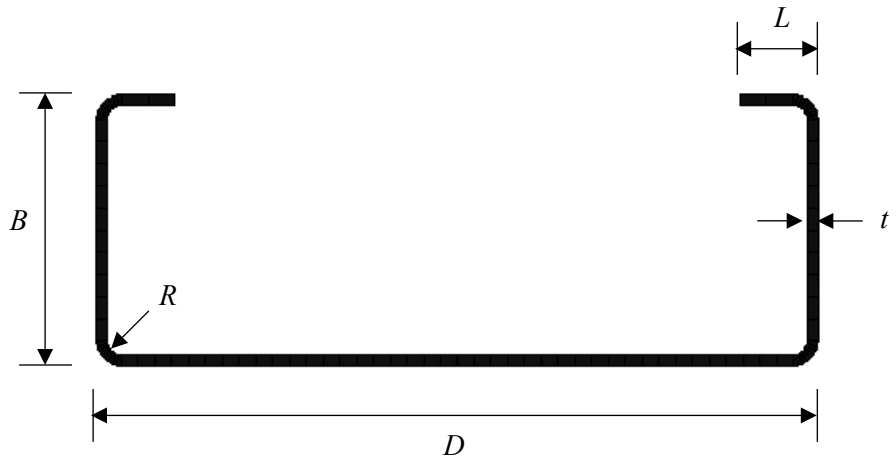

Figure 2: Channel dimension nomenclature.

3 ELASTIC BUCKLING ANALYSIS

The first stage of this research involves performing elastic buckling analyses of channels to investigate their buckling modes. The analysis was conducted using the elastic finite strip buckling analysis program THIN-WALL-2 [6]. THIN-WALL-2 calculates the longitudinal stresses caused by moment and axial load, shear stresses caused by shear load, and normal stresses caused by localised load. The buckling deformations due to these loads are also calculated. THIN-WALL-2 also calculates a graph known as a "signature curve" which shows the variation of the buckling stress with the buckle half-wavelength. The graph is called a signature curve because every section shape displays a unique graph.

A typical signature curve for a cold-formed steel channel under minor axis bending with the lips in compression is shown in Figure 3. It can be seen that the graph displays two minimum points. The first minimum represents the elastic local buckling stress f_{ol} while the second minimum represents the elastic distortional buckling stress f_{od}. For this particular section, the elastic distortional buckling stress is much lower than the elastic local buckling stress, so distortional buckling is the governing failure mode.

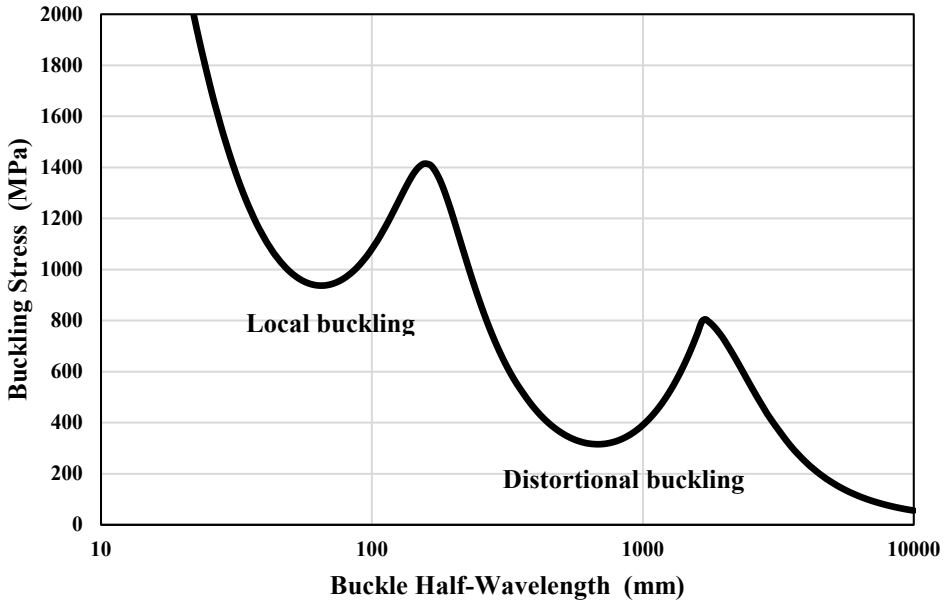

Figure 3: Signature curve for channel under minor axis bending with lips in compression.

Typical local and distortional buckling modes for a channel under minor axis bending with the lips in compression from THIN-WALL-2 are shown in Figures 4 and 5. The local buckling mode involves deformation of the flanges and lips without movement of the junctions between the web and flanges and between the flanges and lips. The distortional buckling mode involves rigid body rotation of the flanges and lips about the web-flange junction combined with deformation of the web.

THIN-WALL-2 can calculate the section properties for thin-walled sections of any shape. For channels under minor axis bending, the program calculates the minor axis section modulus Z_y. This allows the yield moment to be calculated as $M_y = f_y Z_y$ where f_y is the yield stress, and the elastic distortional buckling moment $M_{od} = f_{od} Z_y$. Using these moments, the section slenderness $\sqrt{(M_y/M_{od})}$ can be calculated. The section slenderness is an important quantity used in DSM design equations described later in this paper.

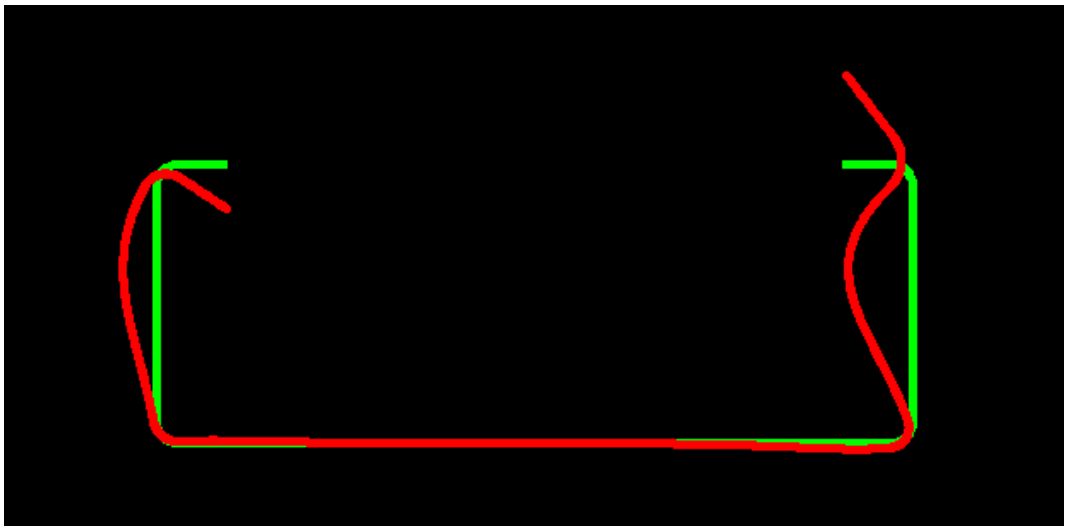

Figure 4: Local buckling mode.

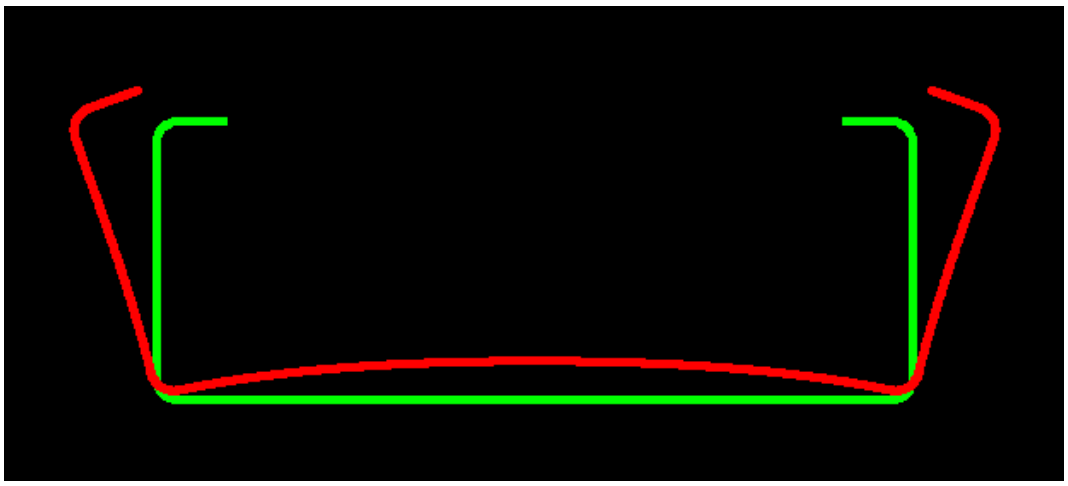

Figure 5: Distortional buckling mode.

An elastic buckling analysis was conducted on all Australian standard cold-formed steel channel sections (plus the additional created channel sections) under minor axis bending with the lips in compression. The results show that the elastic distortional buckling stress f_{od} is less than the elastic local buckling stress f_{ol} for all of these channels. This is displayed graphically in Figure 6, which shows the variation of f_{od}/f_{ol} with D/B and B/L for all the channels analysed

in this research. It can be seen in Figure 6 that the value of f_{od}/f_{ol} is much less than 1.0 for all the channels. Further studies for a wider range of geometries show that f_{od}/f_{ol} is less than 1.0 for all channels except for some very thin channels with very small values of B/L which results in very low local buckling stresses. Thus, it can be concluded that distortional buckling is the governing failure mode for all practical cold-formed steel channels under minor axis bending with the lips in compression.

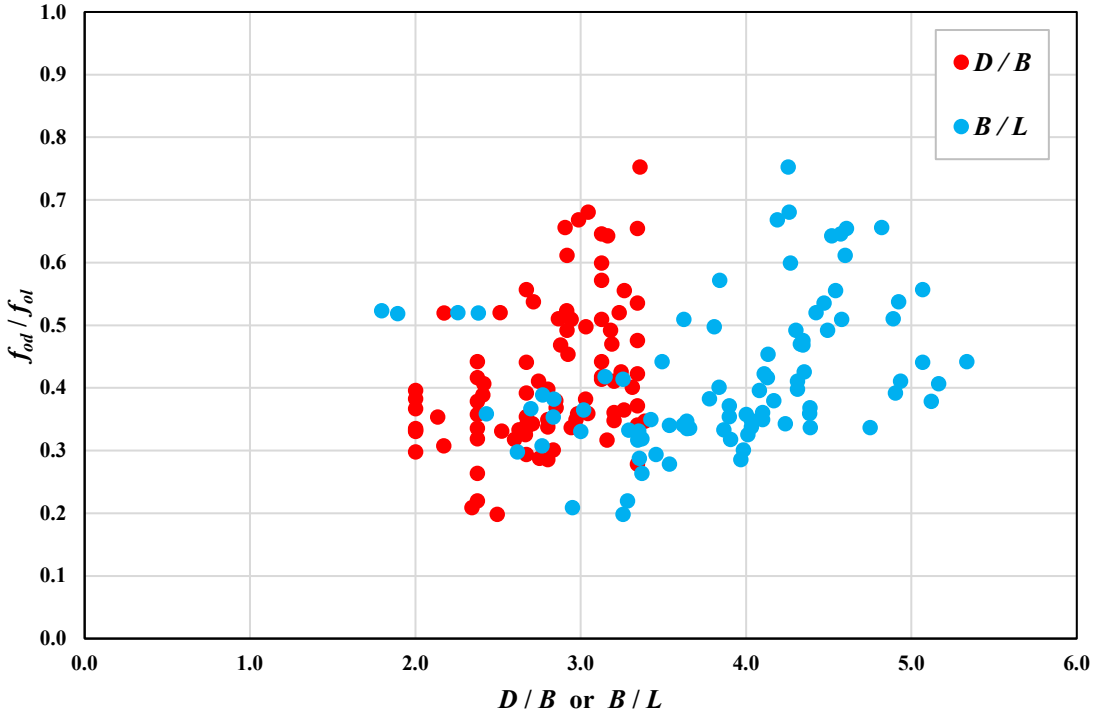

Figure 6: Variation of f_{od}/f_{ol} with D/B and B/L.

4 FINITE ELEMENT MODEL

4.1 Mesh

The commercial finite element analysis software Strand7 [19] was used to conduct a linear buckling analysis and a non-linear static analysis on a range of cold-formed steel channels to calculate the ultimate moment capacity. The non-linear static analysis takes into account material non-linearity and geometric imperfections.

The channel member was created in Strand7 by importing the node coordinates from THIN-WALL-2 and "extruding" the section to the required length using plate (shell) elements. The length of the channel member was selected as $2L_d$ where L_d is the distortional buckling half-wavelength from the signature curve shown in Figure 3. The channel member length is long enough to allow one full distortional buckling wavelength to form but short enough to eliminate the possibility of global buckling. The other reason why a member length of two half-wavelengths was used is so that the effect of both outward and inward geometric imperfections of the flanges and lips can be included in the NLFEA. This will allow the NLFEA to capture the effect of the most detrimental geometric imperfection direction, a phenomenon first identified for inverted hat sections by Martins *et al.* [15].

A convergence study showed that a plate (shell) element mesh size of approximately 5 mm for a 200 mm deep channel is sufficient to yield an accurate result. The finite element model of a cold-formed steel channel is shown in Figure 7.

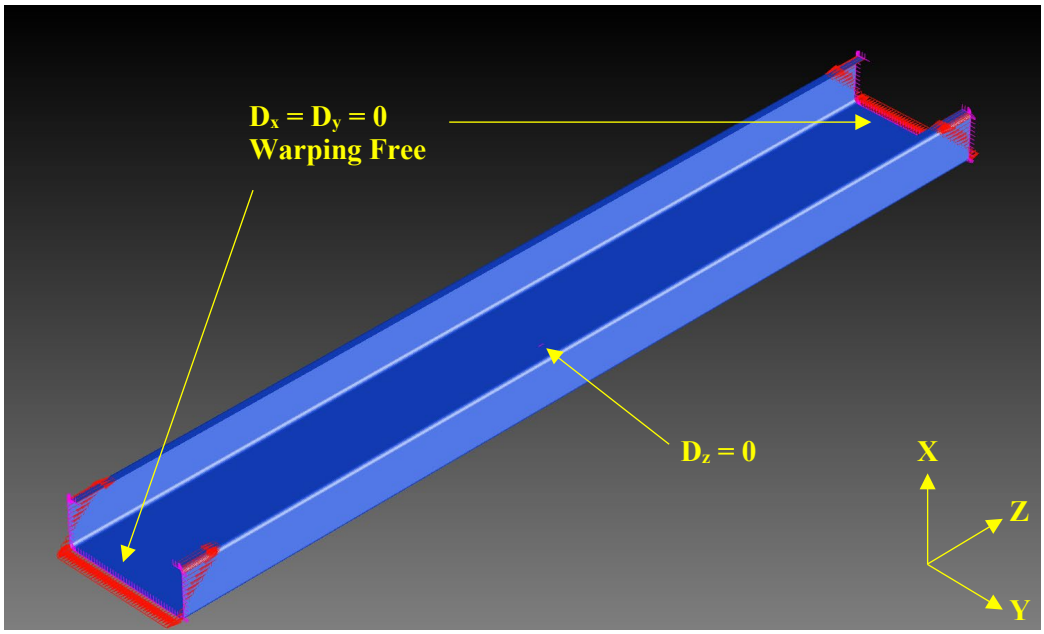

Figure 7: Finite element model of channel.

4.2 Boundary Conditions

The channel beam is simply supported which means the displacements in the vertical X and horizontal Y directions are restrained at each node at both ends but the longitudinal displacement is unrestrained so that the ends are free to warp. At mid-span, the longitudinal displacement is restrained to prevent displacement of the beam in the longitudinal Z direction.

4.3 Load

The load is applied in the form of a global stress gradient at each end of the beam, as shown in Figure 8. The stress gradient is applied in proportion to the vertical X coordinate so that the resultant is a moment with no axial force. This type of loading will simulate equal and opposite end moments acting on the beam which will result in uniform bending.

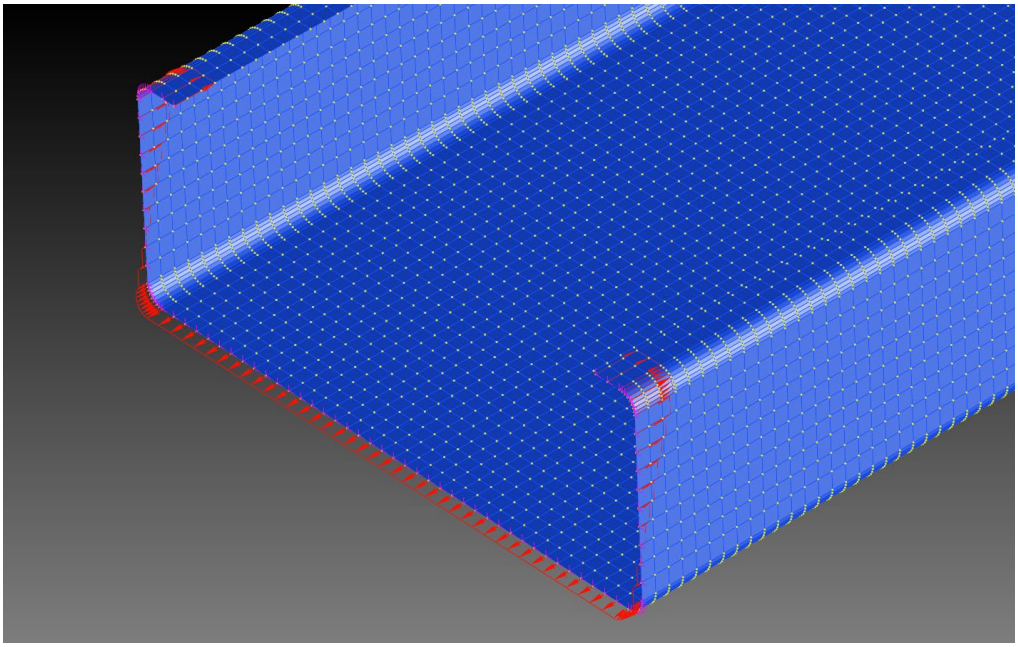

Figure 8: Stress gradient applied at each end of the beam.

4.4 Material Properties

The material properties of the channel sections include the elastic modulus $E = 200{,}000$ MPa and Poisson's ratio $\nu = 0.3$. These are the recommended values given in AS/NZS 4600 [1]. The shear modulus G is calculated as

$$G = \frac{E}{2(1+\nu)} = 76{,}923 \text{ MPa} \quad (1)$$

In Australia, there are three common steel grades available for cold-formed steel depending on the material thickness. Table 1 shows the steel grades and corresponding thickness t, yield stress f_y and ultimate tensile strength f_u. These stresses are used in defining the stress-strain curves of the channel sections for the NLFEA.

Table 1: Steel grades.

Steel grade	t (mm)	f_y (MPa)	f_u (MPa)
G450	≥ 1.5	450	480
G500	$1.0 < t < 1.5$	500	520
G550	≤ 1.0	550	550

The stress-strain curves for the NLFEA were obtained by using the two stage Ramberg-Osgood stress-strain curves for cold-formed steel proposed by Gardner and Yun [20]. From an extensive range of test results, Gardner and Yun derived stress-strain equations which are based only on the three material properties E, f_y and f_u. Using these stress-strain equations, the stress-strain curves for cold-formed steel for the three available Australian steel grades in Table 1 are shown in Figure 9.

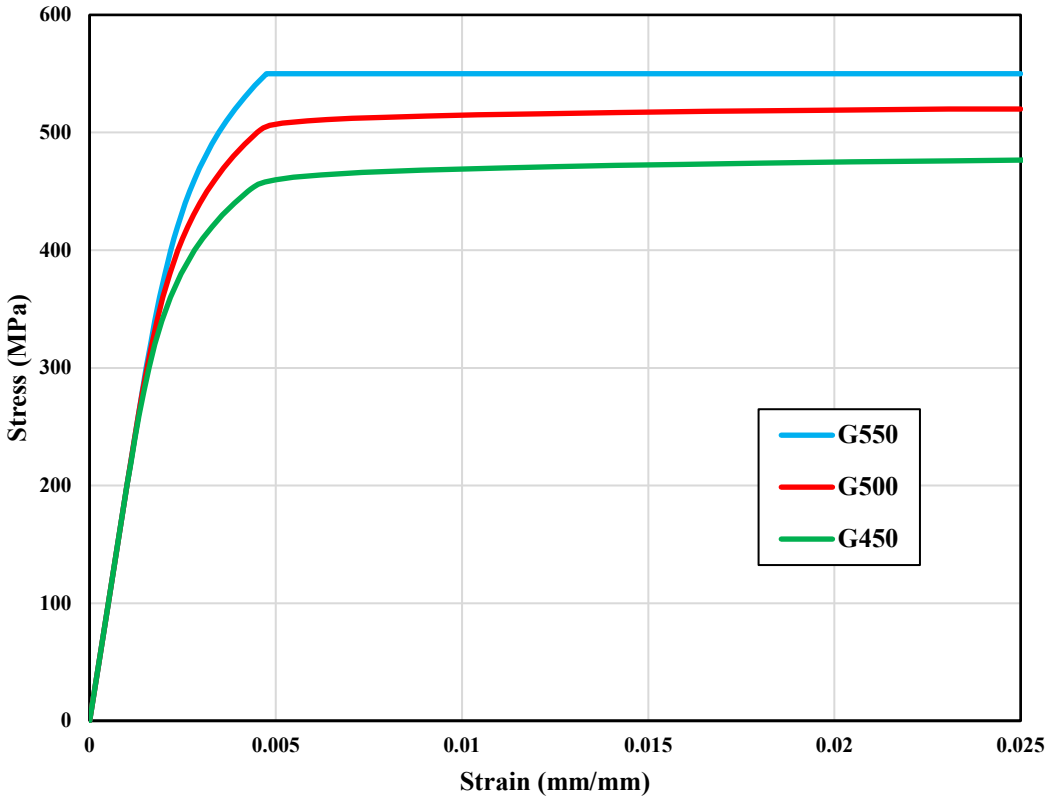

Figure 9: Stress-strain curves for cold-formed steel.

4.5 Geometric Imperfections

The most common method used to model the geometric imperfections is to base the shape of the geometric imperfections on the buckling mode from a linear buckling analysis. The amplitude of the geometric imperfections is scaled up to a certain value which is obtained from previous measurements on cold-formed steel members described by Schafer and Pekoz [21].

For distortional buckling, Schafer and Pekoz proposed that there is a 25% chance of geometric imperfections having an amplitude of 0.64t and a 75% chance of geometric imperfections having an amplitude of 1.55t. For this study, a maximum amplitude of 1.55t is conservatively used for the geometric imperfections, as shown in Figure 10.

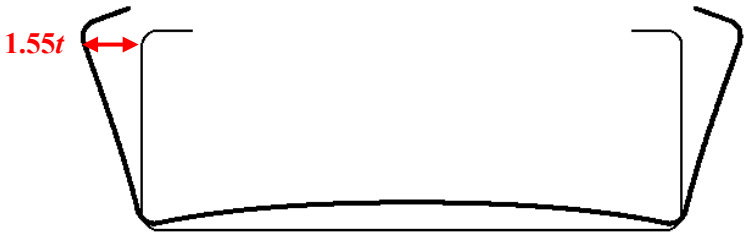

Figure 10: Maximum amplitude of geometric imperfections.

4.6 Validation of Non-Linear Finite Element Analysis

The boundary conditions and applied load are very similar to those used by other researchers including Martins *et al.* [15] for inverted hat sections. The ultimate moments calculated by the NLFEA show very good agreement with the values calculated by Martins *et al.* [15].

5 FINITE ELEMENT LINEAR BUCKLING ANALYSIS

Before running the NLFEA, a linear buckling analysis is conducted in Strand7 to obtain the buckled shape which will be used to model the geometric imperfections. The linear buckling analysis is also used to check that the distortional buckling moment agrees with the value calculated by THIN-WALL-2. This will confirm that the loading and boundary conditions are appropriate for the finite element analysis. Figure 11 shows a typical distortional buckling shape from the linear buckling analysis in Strand7. The distortional buckling moments calculated by Strand7 agree very closely with the values calculated by THIN-WALL-2 for all the channels.

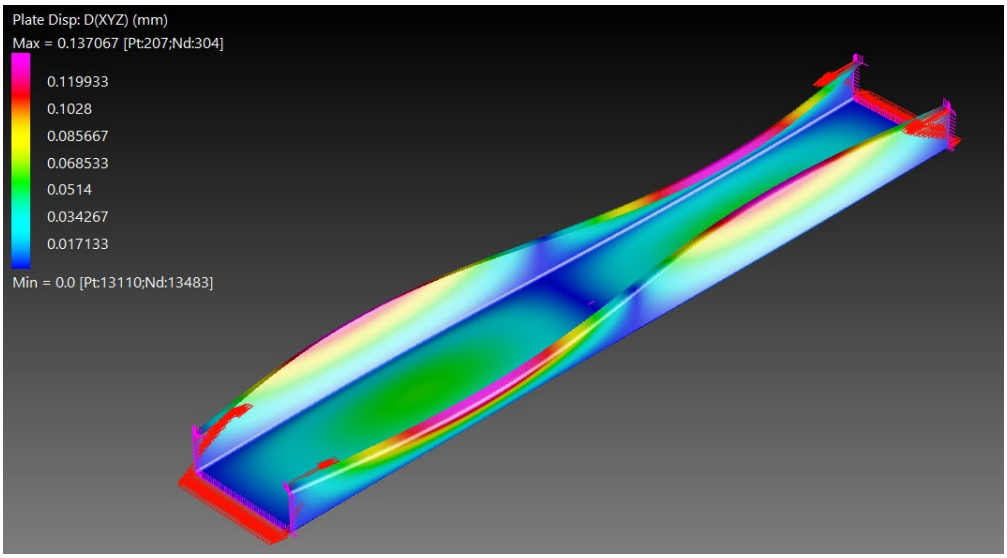

Figure 11: Buckled shape from linear buckling analysis in Strand7.

6 NON-LINEAR FINITE ELEMENT ANALYSIS

In the NLFEA in Strand7, the applied stresses at each end are automatically incremented using a load factor until the maximum load factor is reached. The ultimate moment M_u is calculated by multiplying the maximum load factor by the applied end moment. The applied end moment is the maximum applied stress multiplied by the minor axis section modulus Z_y.

Graphs of normalised moment versus deflection for a C20015 channel (D = 203 mm, t = 1.5 mm) are shown in Figure 12. It can be seen in Figure 12 that the vertical deflection of the channel remains linear until the ultimate moment is nearly reached whereas the horizontal deflection of the flange and lip starts to exhibit non-linear behaviour almost from the outset.

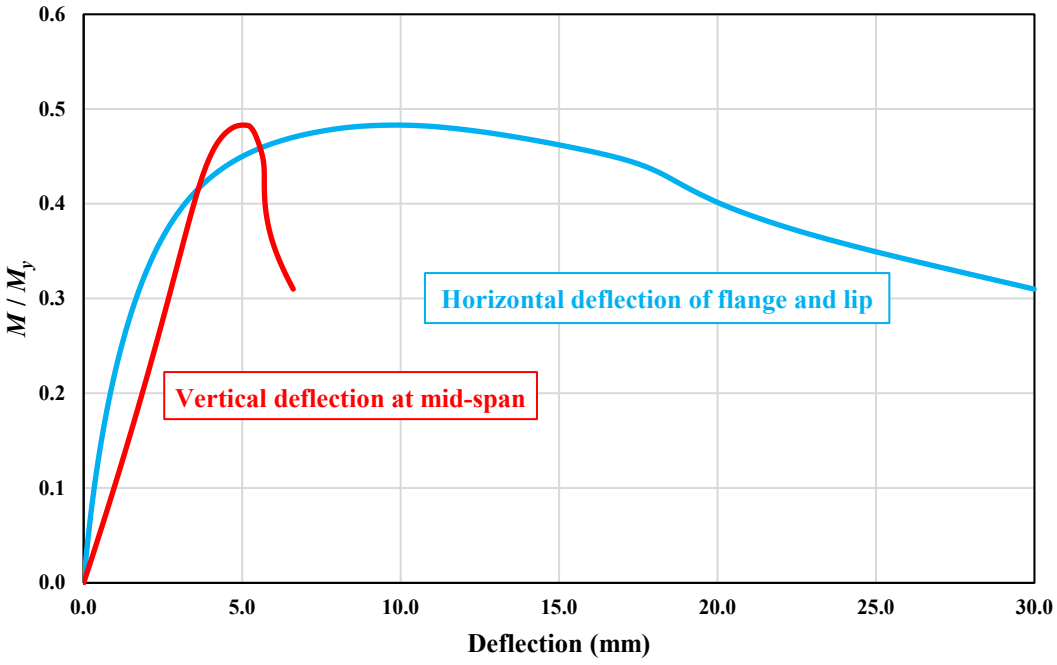

Figure 12: Moment versus deflection.

The longitudinal stress distribution of the C20015 channel at ultimate moment is shown in Figure 13. The stress in the lips where the distortional deformation is occurring has surpassed the yield stress of 450 MPa and so it can be concluded that the channel has failed by inelastic distortional buckling.

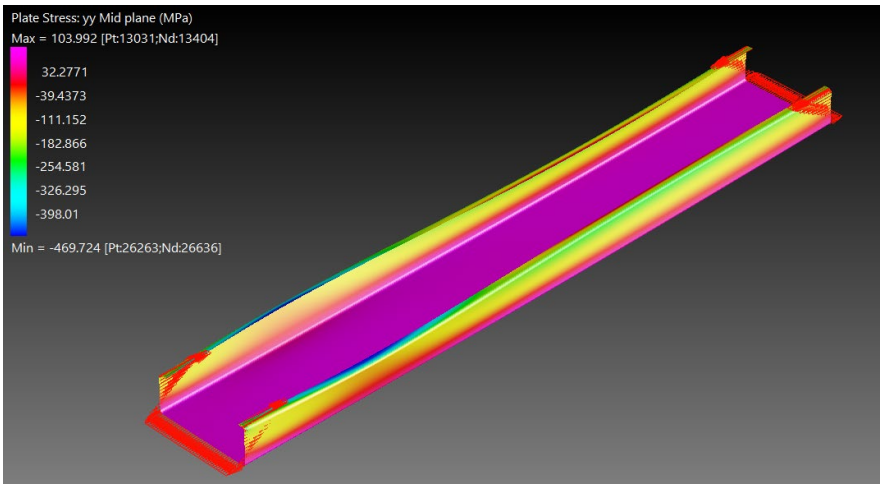

Figure 13: Longitudinal stress distribution at ultimate moment.

The deformed shape of the C20015 channel at post ultimate moment is shown in Figure 14. The inelastic distortional buckling of the channel has evolved into large distortional deformation of the flanges, resulting in high compressive stress in the lips which has caused a local buckle to form in one of the lips.

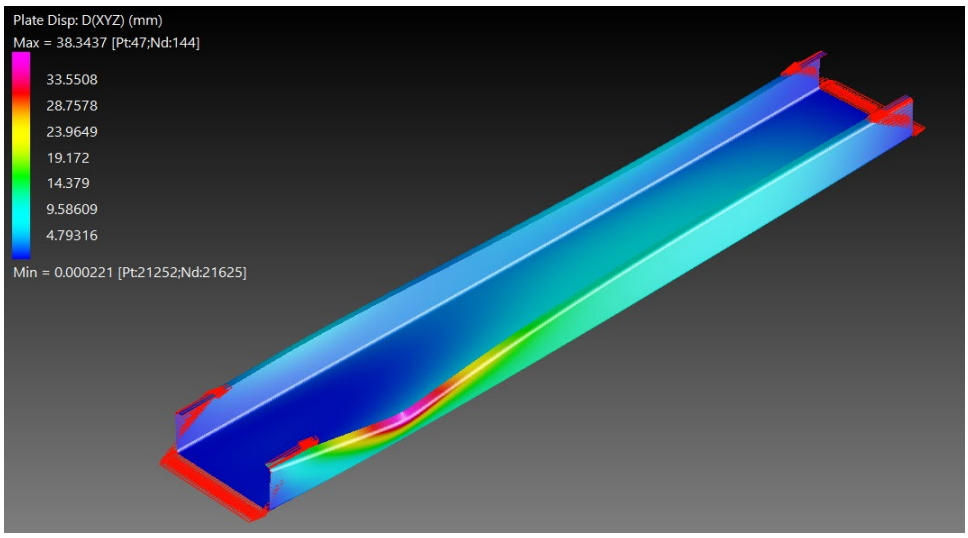

Figure 14: Deformed shape at post ultimate moment.

The ultimate moments for all the channels from the NLFEA normalised with the yield moment M_y can be plotted on a graph as a function of the section slenderness $\sqrt{(M_y/M_{od})}$, as shown in Figure 15. Also shown on the graph is the current DSM design curve and the elastic buckling curve. Although channels with a wide range of values for D/B and B/L were analysed, a well-defined trend can be seen between ultimate moment and section slenderness. Moreover, the graph depicts that the current DSM overestimates the design moment capacity for channels under minor axis bending with the lips in compression. The graph also shows that failure occurs before elastic buckling by inelastic distortional buckling as described earlier in this section.

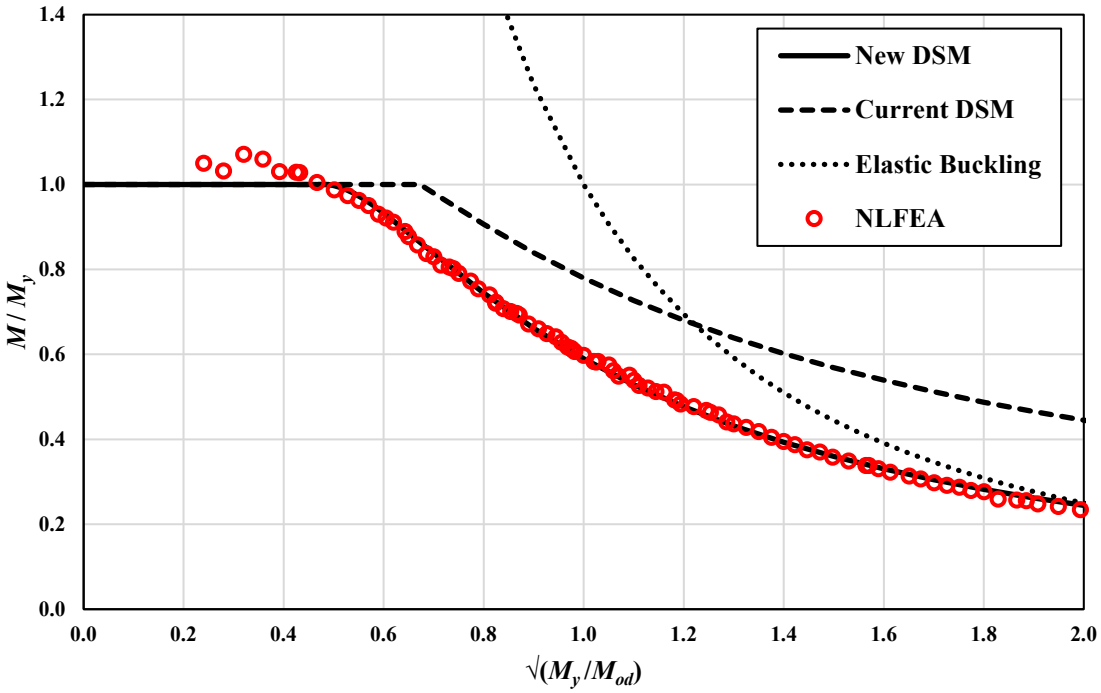

Figure 15: Ultimate moments compared with DSM.

7 PROPOSED DSM DESIGN EQUATION

The current DSM design equation for distortional buckling as described in AS/NZS 4600 [1] and AISI S100 [2] and shown on the graph in Figure 15 can be expressed as

$$\begin{aligned} &\text{For } \lambda_d \leq 0.673: && \frac{M_{bd}}{M_y} = 1.0 \\ &\text{For } \lambda_d > 0.673: && \frac{M_{bd}}{M_y} = \left[1 + a\left(\frac{M_{od}}{M_y}\right)^b\right]\left(\frac{M_{od}}{M_y}\right)^b \end{aligned} \tag{2}$$

where M_{bd} is the design moment capacity, the constants $a = -0.22$ and $b = 0.5$, and λ_d is the section slenderness $\sqrt{(M_y/M_{od})}$. The aim of this research is to derive a similar DSM design equation that best fits the NLFEA results in Figure 15. However, it was found not to be possible to derive a similar equation with just the two constants *a* and *b*. Instead, as was previously done by Martins *et al.* [15] for inverted hat sections, a modified DSM design equation with three constants *a*, *b* and *c* can be derived as

$$\frac{M_{bd}}{M_y} = \left[1 + a\left(\frac{M_{od}}{M_y}\right)^b\right]\left(\frac{M_{od}}{M_y}\right)^c \tag{3}$$

To determine the values of *a*, *b* and *c* which provide the best fit for the above equation to the NLFEA results in Figure 15, the Solver function in Excel was used to calculate *a*, *b* and *c*. This leads to a proposed new DSM design equation shown in Figure 15 which can be expressed as

$$\begin{aligned} &\text{For } \lambda_d \leq 0.485: && \frac{M_{bd}}{M_y} = 1.0 \\ &\text{For } \lambda_d > 0.485: && \frac{M_{bd}}{M_y} = \left[1 - 0.41\left(\frac{M_{od}}{M_y}\right)^{0.36}\right]\left(\frac{M_{od}}{M_y}\right)^{0.81} \end{aligned} \tag{4}$$

To get an indication of how well the proposed DSM design equation fits the NLFEA results in Figure 15, the coefficient of determination R^2 can be calculated. The value of R^2 can range between 0.0 and 1.0, where a value of 1.0 indicates a perfect fit. The value of R^2 was found to be 0.9986 which indicates that the new DSM design equation provides a very accurate fit to the NLFEA results in Figure 15.

8 CONCLUSIONS

Elastic finite strip buckling analysis and non-linear finite element analysis (NLFEA) have been described for cold-formed steel channels under minor axis bending with the lips in compression. The elastic finite strip buckling analysis is performed by the program THIN-WALL-2 while the NLFEA is performed by the program Strand7.

The results of the elastic finite strip buckling analysis reveal that distortional buckling is the governing failure mode for all channels under minor axis bending with the lips in compression. The NLFEA showed that the channels failed by inelastic distortional buckling before the elastic buckling moment is reached.

The ultimate moments calculated by the NLFEA are well below the current DSM design curve. A new DSM design equation was derived which agrees very well with the ultimate moments from the NLFEA.

REFERENCES

[1] Standards Australia and Standards New Zealand, *AS/NZS 4600 – Cold-Formed Steel Structures*, Sydney, Australia, 2018.

[2] American Iron and Steel Institute, *AISI S100 – North American Specification for the Design of Cold-Formed Steel Members*, Washington DC, USA, 2016.

[3] Schafer B.W. and Pekoz T., "Direct strength prediction of cold-formed steel members using numerical elastic buckling solutions", *14th International Specialty Conference on Cold-Formed Steel Structures*, St. Louis, USA, 1998.

[4] Hancock G.J., Kwon Y.B. and Bernard E.S., "Strength design curves for thin-walled sections undergoing distortional buckling", *Journal of Constructional Steel Research*, **31**, 169-186, 1994.

[5] Oey O. and Papangelis J.P., "Behaviour of cold-formed steel channels bent about the minor axis", *Thin-Walled Structures*, **164**, 2001.

[6] Nguyen V.V., Hancock G.J. and Pham C.H., "Development of the THIN-WALL-2 program for buckling analysis of thin-walled sections under generalised loading", *8th International Conference on Advances in Steel Structures*, Lisbon, Portugal, 2015.

[7] Schafer B.W. and Adany S., "Buckling analysis of cold-formed steel members using CUFSM: conventional and constrained finite strip methods", *18th International Specialty Conference on Cold-Formed Steel Structures*, Orlando, USA, 2006.

[8] Cheung Y.K. and Tham L.G., *The Finite Strip Method*, CRC Press, Boca Raton, USA, 1998.

[9] Hancock G.J., "Design for distortional buckling of flexural members", *Thin-Walled Structures*, **27**(1), 3-12, 1997.

[10] Schafer B.W., Sarawit A. and Pekoz T., "Complex edge stiffeners for thin-walled members", *Journal of Structural Engineering*, **132**(2), 212-226, 2006.

[11] Glauz R.S., "Distortional buckling of cold-formed steel flanges under stress gradient", *Journal of Structural Engineering*, **146**(9), 2020.

[12] Yu C. and Schafer B.W., "Simulation of cold-formed steel beams in local and distortional buckling with applications to the direct strength method", *Journal of Constructional Steel Research*, **63**, 581-590, 2007.

[13] Pham C.H. and Hancock G.J., "Direct strength design of cold-formed purlins", *Journal of Structural Engineering*, **135**(3), 229-238, 2009.

[14] Pham C.H. and Hancock G.J., "Experimental investigation and direct strength design of high-strength, complex C-sections in pure bending", *Journal of Structural Engineering*, **139**(11), 1842-1852, 2013.

[15] Martins A.D., Landesmann A., Camotim D. and Dinis P.B., "Distortional failure of cold-formed steel beams under uniform bending: behaviour, strength and DSM design", *Thin-Walled Structures*, **118**, 196-213, 2017.

[16] Fan S., Chen M., Li S., Ding Z., Shu G. and Zheng B., "Stainless steel lipped C-section beams: numerical modelling and development of design rules", *Journal of Constructional Steel Research*, **152**, 29-41, 2019.

[17] Glauz R.S. and Schafer B.W., "Modifications to the direct strength method of cold-formed steel design for members unsymmetric about the axis of bending", *Thin-Walled Structures*, **173**, 2022.

[18] Glauz R.S., "Direct strength method: a fresh new appearance", *CFSRC Colloquium*, USA, 2022.

[19] Strand7, *Finite Element Analysis*, Sydney, Australia, 2023.

[20] Gardner L. and Yun X., "Description of stress-strain curves for cold-formed steels", *Construction and Building Materials*, **189**, 527-538, 2018.

[21] Schafer B.W. and Pekoz T., "Computational modeling of cold-formed steel: characterizing geometric imperfections and residual stresses", *Journal of Constructional Steel Research*, **47**(3), 193-210, 1998.